nature geoscience

LETTERS

PUBLISHED ONLINE: 25 OCTOBER 2009 | DOI: 10.1038/NGEO661

Distribution of melt beneath Mount St Helens and Mount Adams inferred from magnetotelluric data

Graham J. Hill[1,2]*, T. Grant Caldwell[1], Wiebke Heise[1,3], Darren G. Chertkoff[4], Hugh M. Bibby[1], Matt K. Burgess[5], James P. Cull[2] and Ray A. F. Cas[2]

Three prominent volcanoes that form part of the Cascade mountain range in Washington State (USA)—Mounts St Helens, Adams and Rainier—are located on the margins of a mid-crustal zone of high electrical conductivity[1–5]. Interconnected melt can increase the bulk conductivity of the region containing the melt[6,7], which leads us to propose that the anomalous conductivity in this region is due to partial melt associated with the volcanism. Here we test this hypothesis by using magnetotelluric data recorded at a network of 85 locations in the area of the high-conductivity anomaly. Our data reveal that a localized zone of high conductivity beneath this volcano extends downwards to join the mid-crustal conductor. As our measurements were made during the recent period of lava extrusion at Mount St Helens, we infer that the conductivity anomaly associated with the localized zone, and by extension with the mid-crustal conductor, is caused by the presence of partial melt. Our interpretation is consistent with the crustal origin of silicic magmas erupting from Mount St Helens[8], and explains the distribution of seismicity observed at the time of the catastrophic eruption in 1980 (refs 9, 10).

The magnetotelluric method determines the conductivity structure of the crust by using electric currents induced in the earth by natural fluctuations in the Earth's external magnetic field. More precisely, the conductivity (σ) or resistivity ($\rho = 1/\sigma$) is inferred from measurements of the amplitude and phase relationships between the surface electric and magnetic field vectors as a function of period. Previous magnetotelluric data[1–4] from a series of widely spaced lines in southern Washington first showed that a conductive zone, the Southern Washington Cascades Conductor (SWCC), occurs in the region between Mounts St Helens, Adams and Rainier (Fig. 1).

The conductance (or conductivity–thickness product) of a body of conductive rock within a resistive host may also be determined using a related magnetovariation technique[5], which uses the relationship between simultaneous magnetic field measurements at different locations. Magnetovariation measurements[5] later confirmed the extent and location of the SWCC (Fig. 2), but these measurements and other more recent long-period magnetotelluric measurements[11] are too widely spaced to be able to determine details of the magmatic system beneath the volcanoes or their relationship to the SWCC. Here we report results from a detailed magnetotelluricsurvey of a $35 \times 35\,km^2$ area around Mount St Helens and from a line of magnetotelluricmeasurements across the southern part of the SWCC between Mount St Helens and Mount Adams (Fig. 1).

As the period increases, the magnetotelluricphase response, a tensor ($\mathbf{\Phi}$), becomes more sensitive to structure at greater depth and insensitive to any distortion produced by localized heterogeneities near the surface, whereas the amplitude response will be distorted at all periods[12]. For this reason we use the phase tensor $\mathbf{\Phi}$ (represented graphically by an ellipse) to illustrate the magnetotelluricdata and induction vectors[13] (also insensitive to distortion by near-surface heterogeneities) to illustrate the vertical magnetic-field response functions. (See Methods for details.)

Figure 2 shows observed phase-tensor ellipses and induction vectors (real part) at a period of 85 s superimposed on the magnetovariation conductance map[5]. The colour of the ellipses shows the geometric mean (Φ_2) of the maximum and minimum phase differences between the magnetic and electric field, that is, the phase averaged over the inducing field's polarization direction. This parameter provides an indicator of the vertical conductivity gradient, values greater than 45° indicating increasing conductivity with increasing depth. High Φ_2 values occur in the northeastern part of the survey area, in good agreement with the region of high conductance inferred from the magnetovariation measurements[5].

Also shown in Fig. 2 are contours of the phase-tensor skew angle[12] (β), which is a co-ordinate invariant measure of the asymmetry produced in the phase response by asymmetries present in the underlying (three-dimensional, 3D) conductivity distribution. High skew values ($\beta > 4°$) immediately east of Mount St Helens imply that the conductivity structure adjacent to the volcano is asymmetric. An indication of the overall resistivity structure along the profile between Mounts St Helens and Adams can be seen directly in the phase-tensor pseudo-section shown in Fig. 3. Phase values greater than 45° for periods between 3 and 300 s east of Mount St Helens (grey background in Fig. 3) suggest a region of high conductivity in the mid-crust coinciding with the location of the SWCC.

The variation in the orientation of the phase-tensor ellipses in Figs 2 and 3 shows that the conductivity structure around Mount St Helens is 3D. However, the overall orientation of the major ellipse axes on the Mount St Helens–Mount Adams profile (Fig. 3) is roughly east–west, suggesting that the regional conductivity structure strikes approximately north–south. In this situation, a two-dimensional (2D) inversion of the profile data (Fig. 3) will give reasonable results provided that the magnetotelluricdata (in particular the phase) corresponding to an induced current flow perpendicular to the conductivity structure are weighted more strongly in the inversion than the corresponding orthogonal components[14,15].

The data were inverted using both 2D and 3D inverse-resistivity modelling algorithms[16,17] for the profile and a $35 \times 35\,km^2$ area

[1]GNS Science, Lower Hutt, Wellington, New Zealand, [2]Australian Crustal Research Centre, Monash University, Melbourne, Australia, [3]Universidade de Lisboa, CGUL-IDL, Lisbon, Portugal, [4]Crystal Prism Consulting Inc., North Vancouver, British Columbia, Canada, [5]USGS California Water Science Center, San Diego, California, USA. *e-mail: g.hill@gns.cri.nz.

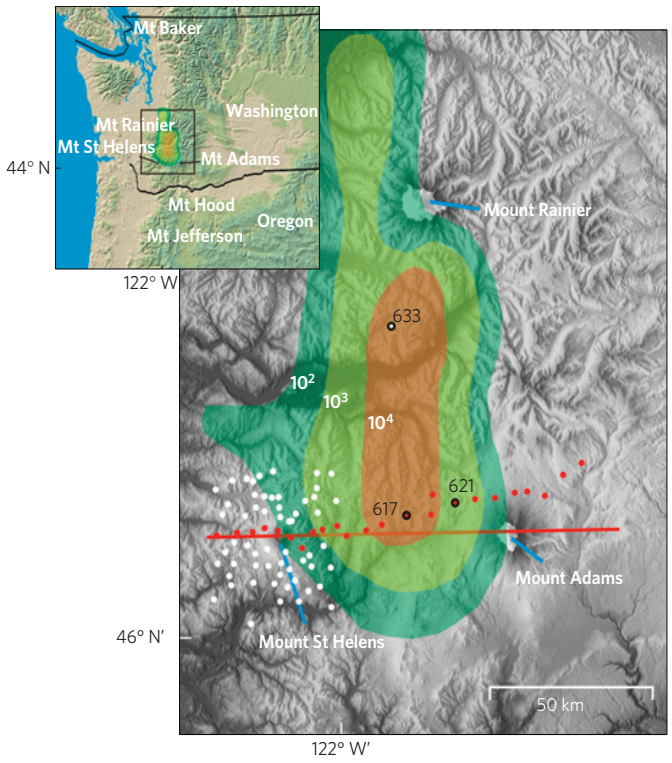

Figure 1 | Locations of magnetotelluricmeasurement sites, Mount St Helens and nearby Cascades volcanoes. The box drawn around Mounts St Helens and Adams in the inset map outlines the area of the magnetotelluricsurvey shown in the adjacent map. White and red dots show the locations of the magnetotelluricmeasurements; measurement sites shown in red were used for the phase-tensor pseudo-section (Fig. 3) and 2D inversion (Fig. 4a). The east–west line (red) shows the profile onto which these measurements were projected. The coloured area shows the region of high conductance[5]. The green-to-orange transition corresponds to the 3×10^3 S contour in Fig. 2.

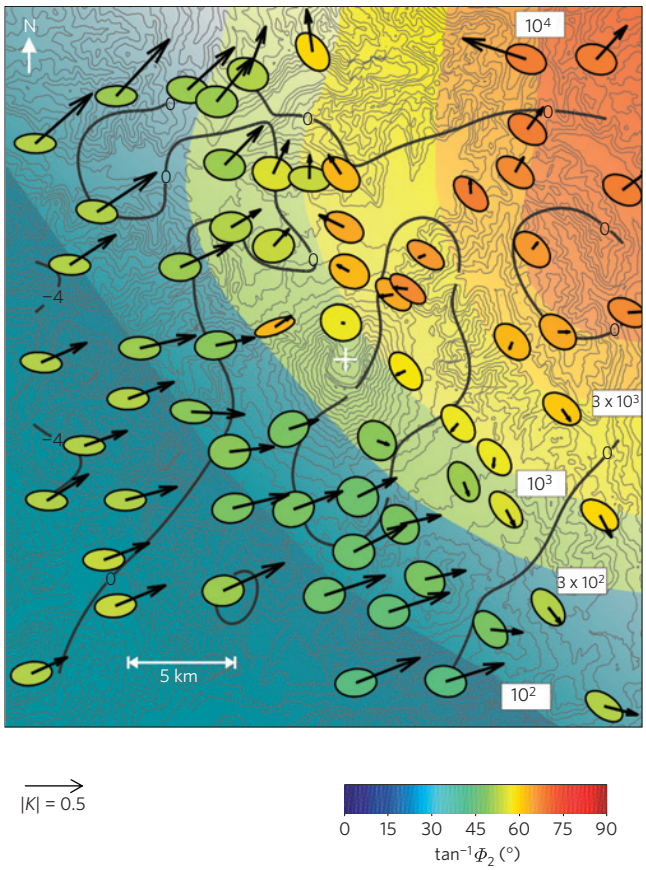

Figure 2 | Phase-tensor ellipses and induction vectors (real parts) at a period of 85.3 s. The background colour shows the SWCC conductance anomaly[5]. Background contours show the topography (contour interval 100 m) centred on Mount St Helens. The phase-tensor ellipses have been normalized by the maximum phase value, with the ellipse colour indicating the geometric mean (Φ_2) of the maximum and minimum phases. Foreground contours show the phase-tensor skew angle. Note the area of high skew angle (>4°) offset just east of the volcano. This feature is a result of the connection of the magma conduit beneath Mount St Helens to the mid-crustal conductor that we identify with the SWCC (refs 1, 2).

shown respectively in Figs 1 and 2. Both algorithms seek to find a resistivity model that fits the data with a minimum amount of model structure or 'roughness' (Supplementary Methods).

The most striking feature of the inverse 2D resistivity model (Fig. 4) is the conductor beneath Mount St Helens that extends eastward to Mount Adams and downwards to join a thick tabular conductive zone at about 15 km depth. This mid-crustal conductor corresponds well with the location of the SWCC in this region. A broad zone of high conductivity, also connected to the mid-crustal conductor, occurs beneath Mount Adams. The robustness of the 2D inversion near Mount St Helens was tested by removing the station from within the crater above the conductor and by inverting data from a SW–NE line through the volcano. The two tests produce similar models (Supplementary Figs. S4 and S5).

The features seen in the 2D model are reproduced by the 3D inversion and the agreement between the 2D and 3D model cross-sections (Fig. 4) is good given the differences in model geometry and discretization (much coarser in the 3D model). However, as can be seen in the depth slices (Fig. 4c–e), the 3D model shows that the localized area of high conductivity under Mount St Helens becomes a 15-km-long dyke-like feature at deeper levels before merging with the mid-crustal conductor at ~15 km depth.

To check the robustness of the 3D inversion, the forward response of a simplified version of the inverse model was calculated[18], omitting the small areas of high conductivity that occur adjacent to the main conductive features (Supplementary Fig. S7). This simplified model reproduces the main features of the observed phase response, suggesting that the small areas of high conductivity are not well constrained by the data and have little or no significance.

The connection between the high-conductivity region beneath the volcano and the edge of the mid-crustal conductor in the northeast will promote downward current flow into the mid-crustal conductor, leading to an asymmetric phase response at long periods. This connection provides an explanation for the asymmetric phase response (skew angles > 4°) observed adjacent to Mount St Helens (Fig. 2). We tested this explanation by calculating[18] phase tensors for simple 3D models of the conductivity structure with and without the link between near-surface and deep conductors. Breaking the link changes the phase response drastically; only a continuous conductive pathway produces an asymmetric response similar to that observed (Supplementary Fig. S8).

The magnetotelluricmeasurements reported here were made during a period of active magma extrusion and the obvious interpretation is that the vertical conductive zone beneath Mount St Helens marks the magma conduit supplying the volcano. The location of the conductive zone is consistent with the location of the shallow melt zone under the volcano inferred from seismicity[9,10] and tomographic inversions of earthquake data[19,20]. The connection between the vertical conductor beneath Mount St Helens and

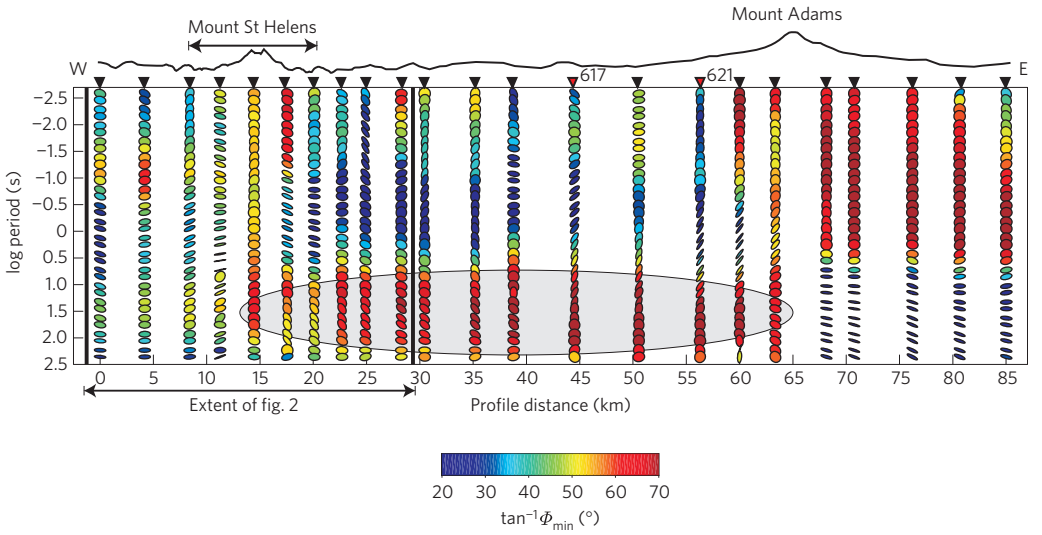

Figure 3 | Phase-tensor ellipse pseudo-section for the east–west line of measurements across the SWCC. The ellipses are plotted so that the horizontal axis corresponds to an east–west orientation. The zone (grey background) where the minimum phase is >50° corresponds to the SWCC (Fig. 2) and the mid-crustal conductive zone in the resistivity models (Fig. 4). The phase signature of the magma conduit beneath Mount St Helens can be seen as a column of nearly circular ellipses beneath the crater with large-eccentricity ellipses to either side. A similar pattern occurs beneath Mount Adams. High phases east of Mount Adams are a consequence of a near-surface layer of high conductivity (Fig. 4).

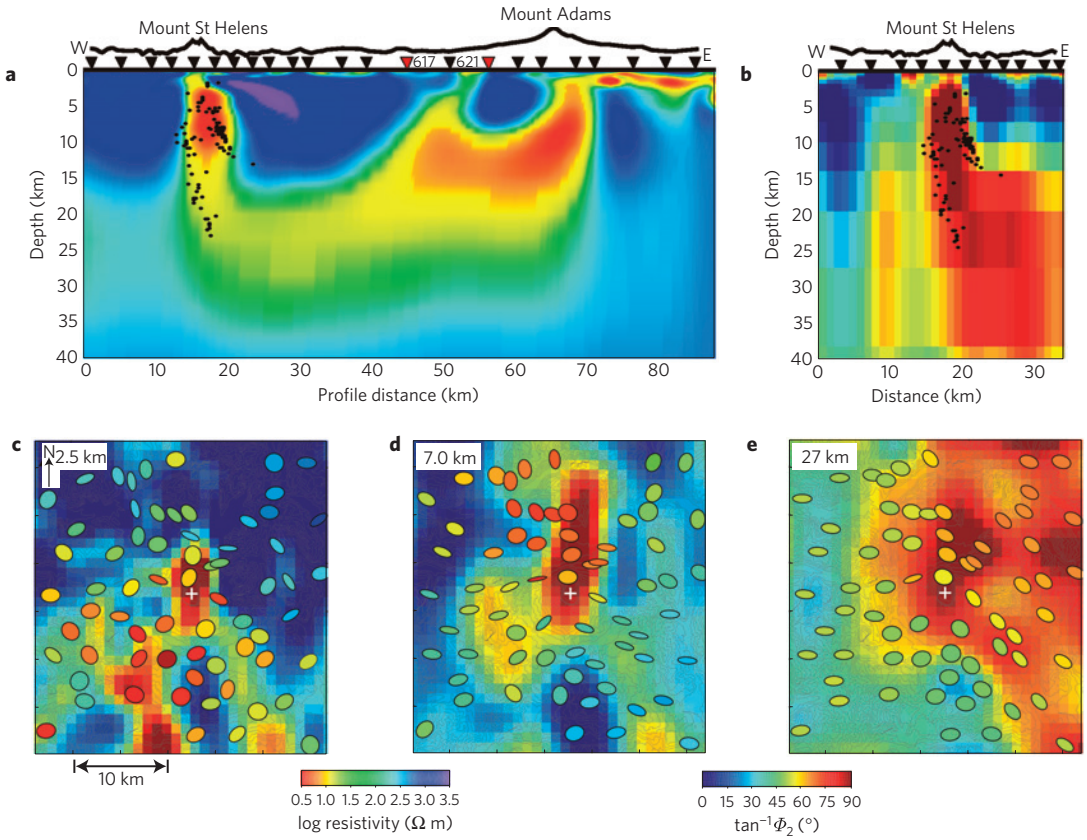

Figure 4 | Resistivity models. a, 2D resistivity model of the east–west line of magnetotelluric measurements across the zone of high conductance shown in Fig. 1. **b–e**, 3D resistivity model derived from the magnetotelluricdata in a 35 × 35 km^2 area around Mount St Helens. **b**, The resistivity along an east–west cross-section though the centre of Mount St Helens. The black dots in **a**,**b**, show the earthquake hypocentres recorded during the 1980 eruption[9]. **c–e**, Depth slices with observed phase tensors at periods of 0.1, 1.8 and 85 s respectively approximately corresponding to the depths of the slices.

the mid-crustal conductor northeast of the volcano suggests that the high conductivity in the mid-crustal conductor is also a consequence of the presence of an interconnected melt fraction between ~2 and 12% (see Supplementary Discussion).

The SWCC has previously been interpreted[1–5] as an eastward-dipping band of conductive marine sediments trapped during accretion at the continental margin. This interpretation is based on one-dimensional modelling at widely spaced measurement

sites, which were then stitched together. We see no evidence of an eastward-dipping high-conductivity zone in our 2D and 3D modelling. High seismic velocities beneath the northern part of the SWCC are also inconsistent with the presence of marine sediments at depths between 10 and 20 km (ref. 21).

Another possible explanation for the high conductance in the SWCC is the presence of an interconnected network of aqueous fluid at the grain boundaries of the rock matrix. The most abundant xenoliths (gabbros) found in the Mount St Helens eruptives show evidence of penetration by water-rich fluids before their incorporation (and partial melting) in the 1980 magma[22]. However, it was concluded[22] that these xenoliths originated at much shallower depths than the source of the Mount St Helens' dacites. The presence of quenched residual melt in some xenoliths demonstrates that high-temperature basaltic melt resides in the lower reaches of the magma reservoir[23]. This makes the existence of a separate aqueous phase at deeper levels unlikely, as its presence would promote melting.

The mid-crustal zone of partial melt suggested by the conductivity structure (Fig. 4) provides a consistent explanation for key features seen in the petrology and seismicity. Eruptive products at Mount St Helens vary compositionally from basalt to dacite[8], the range reflecting mixing between mafic and silicic magmas[8,24]. The origin of the dacitic magma at Mount St Helens has been attributed to either partial melting of the lower crust[25] or melting of the underlying subducting slab[26]; the basaltic component originates from partial melting of the mantle wedge[27]. The conductivity structure (Fig. 4) suggests that the dacitic magmas erupted from Mounts St Helens and Adams originate from a large zone of partial melt within the mid-crust rather than the slab.

The locations of earthquakes[9] recorded near Mount St Helens at the time of the 1980 eruption are concentrated near the margins of the conductive zone (Fig. 4). The seismicity extends more deeply in the west than in the east, where it terminates near the top of the mid-crustal conductor. A zone of partial melt is expected to be aseismic owing to the weakening effect of the melt fraction consistent with the lack of earthquakes located within the conductive zone. The seismicity observed at the time of the eruption would be expected at the margins of the melt zone, where the shear stress between the rising magma and surrounding rock would be greatest. The interpretation that the high-conductivity zone at ~15 km depth northeast of the volcano is due to partial melt thus neatly explains the difference in the depth extent of the seismicity east and west of the volcano.

The mid-crustal conductive zone below ~15 km (Fig. 4) corresponds to the location of the SWCC (refs 1–5) in the area east and northeast of Mount St Helens (Figs 1 and 2). A single magnetotelluricsounding made just south of Mount Rainier (site 633, Fig. 1) has a similar phase response to soundings between Mounts St Helens and Adams. This raises the possibility that the entire SWCC marks a single laterally extensive zone of partial melt in the mid-crust. High heat-flow values[28] measured in the area of the SWCC provide support for this possibility. A zone of partial melt extending northward from Mount St Helens to near Mount Rainier would be comparable in area to the largest silicic volcanic systems known[23] (for example the Taupo Volcanic Zone in New Zealand[29], also underlain by a mid-crustal conductor[30]). More broadband magnetotelluricdata and other geophysical investigations in the wider region of the SWCC are required to further test the possibility that the whole SWCC marks a layer of partial melt.

Methods

The magnetotelluricamplitude and phase relationships used to determine the subsurface conductivity structure are expressed by frequency-domain or period-dependent transfer functions between the various components of the electromagnetic field measured at the surface. Details of the instrumentation and data processing used for these measurements are given in Supplementary Methods.

The (complex) transfer functions take the form of an 'impedance tensor **Z**' defined by the relation $\mathbf{E} = \mathbf{ZH}$ between the horizontal components of the electric- (**E**) and magnetic- (**H**) field vectors, and an induction vector **K** defined by the scalar product $-\mathbf{K}\cdot\mathbf{H} = H_z$, where H_z is the vertical magnetic field component and **K** has been defined[13] so that the vector points in the direction of increasing conductance. These functions represent the normalized inductive response of the earth to the fluctuations in the earth's external magnetic field. In simple layered or quasilayered situations, skin depth $\approx 0.5\sqrt{(\rho T)}$ in kilometres (where T is the period and ρ is some representative measure of the overlying resistivity) can be used as a crude estimate of detection depth.

The information contained in the impedance tensor for conductivity variations at depth is contained in the phase and shape of the amplitude response as a function of period rather than the amplitude or magnitude response, which is subject to distortion by localized near-surface conductivity heterogeneities[12]. As the phase response is free of the distortion in the electric field produced by such heterogeneities (known as galvanic distortion), it provides a way of visualizing the magnetotelluricresponse from depth without many of the complications produced by near-surface structure. The magnetotelluric phase response is represented by the tensor $\mathbf{\Phi} = \mathbf{X}^{-1}\mathbf{Y}$, where **X** and **Y** are the 2×2 matrices representing the real and imaginary parts of **Z**. It is easy to show that $\mathbf{\Phi}$ is independent of galvanic distortion[12]. As **K** does not depend directly on the electric field it is also less sensitive to galvanic distortion than the amplitude response contained in **Z**.

Graphically, the phase tensor ($\mathbf{\Phi}$) is represented by an ellipse[12]. This can be coloured in different ways to emphasize different aspects of the response, providing a distortion-free way of visualizing aspects of the conductivity structure at depth directly from the (period-domain) data. For example, in a simple 2D situation the orientation of the ellipse axes (that is, the principal axes of the tensor) indicates the direction of steepest horizontal conductivity gradient or its normal in a similar fashion to the induction vectors[12].

In general, $\mathbf{\Phi}$ is symmetric only where the conductivity structure around the measurement site is symmetric. For example, if the conductivity is 2D (that is, mirror symmetric), $\mathbf{\Phi}$ is symmetric. The departure of $\mathbf{\Phi}$ from symmetry is thus a measure of the asymmetry present in the underlying conductivity structure, which can be expressed by the skew angle $\beta = 0.5\tan^{-1}[(\Phi_{12} - \Phi_{21})/(\Phi_{11} + \Phi_{22})]$. In a 2D, or quasi-2D, situation, where β is zero or small (respectively), the phase-tensor ellipse will have either its major or minor axes aligned with the 'geoelectric' strike direction.

Although the phase response is sensitive to changes in conductivity, information on the magnitude of the amplitude response (usually represented by an apparent resistivity) is required before the geometry and resistivity of the conductivity structure can be determined. Because of this requirement (regularized) nonlinear inversions[16,17] of the magnetotelluricdata must be used to construct images of the subsurface resistivity (see Supplementary Methods for details).

Received 24 April 2009; accepted 23 September 2009; published online 25 October 2009

References

1. Stanley, W. D. Tectonic study of the Cascade Range and Columbia Plateau in Washington based on magnetotelluric soundings. *J. Geophys. Res.* **89,** 4447–4460 (1983).
2. Stanley, W. D., Finn, C. A. & Plesha, J. L. Tectonics and conductivity structures in the southern Washington Cascades. *J. Geophys. Res.* **92,** 10179–10193 (1987).
3. Stanley, W. D., Mooney, W. D. & Fuis, G. S. Deep crustal structure of the Cascade Range and surrounding regions from seismic refraction and magnetotelluric data. *J. Geophys. Res.* **95,** 19419–19438 (1990).
4. Stanley, W. D., Johnson, S. Y., Qamar, A. I., Weaver, C. S. & Williams, J. M. Tectonics and seismicity of the Southern Washington Cascade Range. *Bull. Seismol. Soc. Am.* **86,** 1–18 (1996).
5. Egbert, G. D. & Booker, J. R. Imaging crustal structure in south western Washington with small magnetometer arrays. *J. Geophys. Res.* **98,** 15967–15986 (1993).
6. Gaillard, F. & Marziano, G. I. Electrical conductivity of magma in the course of crystallization controlled by their residual liquid composition. *J. Geophys. Res.* **110,** B06204 (2005).
7. ten Grotenhuis, S. M., Drury, M. R., Spiers, C. J. & Peach, C. J. Melt distribution in olivine rocks based on electrical conductivity measurements. *J. Geophys. Res.* **110,** B12201 (2005).
8. Gardner, J. E., Carey, S., Sigurdsson, H. & Rutherford, M. J. Influence of magma composition on the eruptive activity of Mount St Helens, Washington. *Geology* **23,** 523–526 (1995).
9. Scandone, R. & Malone, S. D. Magma supply, magma discharge and readjustment of the feeding system of Mount St Helens during 1980. *J. Volcanol. Geotherm. Res* **23,** 239–262 (1985).
10. Musumeci, C., Malone, S. D. & Gresta, E. Magma system recharge of Mount St Helens (USA) from precise relative hypocenter location of microearthquakes. *J. Geophys. Res.* **107,** 2264 (2002).
11. Patro, P. K. & Egbert, G. D. Regional conductivity structure of Cascadia: Preliminary results from 3D inversion of USArray transportable array magnetotelluric data. *Geophys. Res. Lett.* **35,** L20311 (2008).

12. Caldwell, T. G., Bibby, H. M. & Brown, C. The magnetotelluric phase tensor. *Geophys. J. Int.* **158,** 457–469 (2004).
13. Parkinson, W. D. The influence of continents and oceans on geomagnetic variations. *Geophys. J. R. Astron. Soc.* **6,** 441–449 (1962).
14. Wannamaker, P. E. *et al.* Fluid generation and pathways beneath an active compressional orogen, the New Zealand Southern Alps, inferred from magnetotelluric data. *J. Geophys. Res.* **107,** 2117 (2002).
15. Booker, J. R., Favetto, A. & Pomposiello, M. C. Low electrical resistivity associated with plunging of the Nazca flat slab beneath Argentina. *Nature* **429,** 399–403 (2004).
16. Rodi, W. & Mackie, R. Non-linear conjugate gradient algorithm for 2D magnetotelluric inversion. *Geophysics* **66,** 174–178 (2001).
17. Siripunvaraporn, W., Egbert, G., Lenbury, Y. & Uyeshima, M. Three-dimensional magnetotelluric: Data space method. *Phys. Earth Planet. Inter.* **150,** 3–14 (2005).
18. Mackie, R. L., Smith, J. T. & Madden, T. R. Three-dimensional electromagnetic modelling using finite difference equations: The magnetotelluric example. *Radio Sci.* **29,** 923–935 (1994).
19. Lees, J. M. & Crosson, R. S. Tomographic inversion for three-dimensional velocity structure at Mount St Helens using earthquake data. *J. Geophys. Res.* **94,** 5716–5728 (1989).
20. Lees, J. M. The magma system of Mount St Helens: Non-linear high resolution P-wave tomography. *J. Volcanol. Geotherm. Res.* **53,** 103–116 (1992).
21. Miller, K. C. *et al.* Crustal structure along the west flank of the Cascades, western Washington. *J. Geophys. Res.* **102,** 17857–17873 (1997).
22. Heliker, C. Inclusions in Mount St Helens dacite erupted from 1980 through 1983. *J. Volcanol. Geotherm. Res.* **66,** 115–135 (1995).
23. Bachmann, O. & Bergantz, G. The magma reservoirs that feed supereruptions. *Elements* **4,** 17–21 (2008).
24. Pallister, J. S., Hoblitt, R. P., Crandell, D. R. & Mullineaux, D. R. Mount St Helens a decade after the 1980 eruptions: Magmatic models, chemical cycles, and a revised hazards assessment. *Bull. Volcanol.* **54,** 126–146 (1992).
25. Smith, D. R. & Leeman, W. P. Petrogenesis of Mount St Helens dacitic magmas. *J. Geophys. Res.* **92,** 10313–10334 (1987).
26. Defant, M. F. & Drummond, M. S. Mount St Helens: Potential example of the partial melting of the subducted lithosphere in a volcanic arc. *Geology* **21,** 547–550 (1993).
27. Leeman, W. P., Smith, D. R., Hildreth, W., Palacz, Z. & Rogers, N. Compositional diversity of late Cenozoic basalts in a transect across the Southern Washington Cascades: Implications for subduction zone magmatism. *J. Geophys. Res.* **95,** 19561–19582 (1990).
28. Blackwell, D. D., Steele, J. L., Kelley, S. & Korosec, M. A. Heat flow in the state of Washington and thermal conditions in the cascade range. *J. Geophys. Res.* **95,** 19495–19516 (1990).
29. Wilson, C. J. N. *et al.* Volcanic and structural evolution of Taupo Volcanic Zone, New Zealand: A review. *J. Volcanol. Geotherm. Res.* **68,** 1–28 (1995).
30. Heise, W. *et al.* Melt distribution beneath a young continental rift: The Taupo Volcanic Zone, New Zealand. *Geophys. Res. Lett.* **34,** L14313 (2007).

Acknowledgements

We would like to thank W. Siripunvarporn for the use of his 3D inverse modelling code WSINV3DMT. B. Schaefer is thanked for the many discussions and support he lent to the completion of the work. The Yakama Nation, Weyerhaeuser, Olympic Resource Management and the US Forest Service are thanked for allowing us access to their land during the course of data collection. The logistical support of L. Mastin (Cascades Volcano Observatory—USGS), E. Rose and G. Barker is gratefully appreciated. We would like to thank E. Castleberry, J. Ellison, A. Fisher, T. Fisher, A. Green, J. Hill, Q. Jordan-Knox, V. Maris, M. McKenna, M. McLean, N. Olivier and L. Wan for help with data collection during the two field campaigns. H. Brasse and G. Jiracek provided reviews of the manuscript.

Author contributions

G.J.H. designed the experiment. G.J.H., T.G.C. and D.G.C. wrote the paper. G.J.H. and W.H. reduced the observed time series. G.J.H., T.G.C., W.H. and H.M.B. carried out the modelling. G.J.H., M.K.B., D.G.C., W.H. and R.A.F.C. carried out the field campaign. All authors contributed to the interpretation and manuscript editing.

Additional information

Supplementary information accompanies this paper on www.nature.com/naturegeoscience. Reprints and permissions information is available online at http://npg.nature.com/reprintsandpermissions. Correspondence and requests for materials should be addressed to G.J.H.